

Numerical Simulation of Axisymmetric and Asymmetric Extrusion Process Using Finite Element Method

S. T. Oyinbo, O.M Ikumapayi, J.S Ajiboye, S.A Afolalu

ABSTRACT: *The deformation load is the most important parameter in the press design. The flow of metal, consequently load, is largely influenced by the geometry of the die and hence the geometric shape of the tools is the main factor by which an optimum load can be developed. In extrusion process the strain distribution, resulting from deformation load, and other important variables that influence material structure, such as a hydrostatic stress, are strongly dependent on the geometry of the die. In the present investigation using linearly converging die profiles, the extrusion of simple and advanced polygons such as circular, square, triangular, hexagonal, heptagonal, octagonal, L-, T-, and H- sections from round billet have been numerically simulated. Mathematical equations describing the die profiles were evaluated. A solid CAD model for the linearly converging die profile was made using Autodesk Inventor 2013 software and numerical analysis using DEFORM 3D software for extrusion of the above sections from round billet was then performed to determine, for dry and lubricated condition, the load prediction, effective stress, effective strain, strain rate, velocity and temperature distribution during the deformation. It is found that the predictive loads for advance (asymmetric) shapes are found to be higher than that of the simple shapes. While there is no marked difference between the predictive load for simple (axisymmetric) shapes, the L-section has the highest extrusion load, followed by T-section and the H-section given the least pressure.*

Keywords: Numerical Simulation; Die Profile; Deformation; Asymmetric and Axisymmetric Extrusion; Finite Element Modeling.

1.0 INTRODUCTION

With the rapid growth of industrialization and technology, the necessity of metal forming operations have increased manifold. In contrast to other manufacturing requirements, the metal forming operation enjoys certain advantages in terms of improved mechanical properties of the product as well as minimization wastage of material in terms of scrap. Extrusion process plays a major role in massive metal deformation process in which cross-sectional area of billet is reduced by pushing with a ram and squeezing through a die. Very often many empirical rules are followed to determine process parameters, extrusion load and geometries of die profiles. However, empirical relations have limited applications and cannot be applied universally under various conditions. A great deal of research have been carried out by different investigators in the recent decades to understand the complex mechanism of metal deformation process in the extrusion process both for two dimensional and three dimensional process

- S.T Oyinbo is an MSc holder in Mechanical Engineering Department, University of Lagos, Akoka, Lagos -State, Nigeria. talk2oyinsun@yahoo.com.
- O.M Ikumapayi is a researcher in Mechanical Engineering Department and MSc holder, University of Lagos, Akoka, Lagos, Nigeria. ikumapayi.omolayo@gmail.com
- J.S Ajiboye is currently an Associate Professor in Mechanical Engineering, University of Lagos, Akoka, Lagos, Nigeria. isajiboye@unilag.edu.ng, or joesehinde@yahoo.com
- S.A Afolalu is currently pursuing a PhD degree program in Mechanical Engineering Department, Federal University of Agriculture Abeokuta Ogun-State, Nigeria. afoniran@yahoo.com

It is evident that geometry of dies plays the most critical role in controlling the extrusion process parameters in case of conventional tapered dies. During the last decade, considerable attention has been directed towards the use of mathematically contoured curved dies for extrusion.

The basic advantage in the use of such dies lies in the fact that there is smooth flow of metal, less redundant work and less deformation load. In the past conical dies are preferred to mathematically contoured dies because of their ease of manufacture. However, now-a-days, the manufacture of mathematically contoured dies has become much easier because of availability of sophisticated computer numerical control machines. The variables influencing an extrusion process are: (i) the percentage of area reduction, (ii) the die geometry, (iii) the product geometry, (iv) the speed of extrusion, (v) the billet temperature, and (vi) lubrication. In a manufacturing situation the above parameters should be suitably optimized to achieve the best results. The ram speed and temperature have major influence on plastic properties of the billet material and their effect can be studied by choosing a suitable constitutive equation. But the effect of reduction, die and product geometry on stresses and strains is rather difficult and this has remained an active area of research for the past few decades.

1.1 Extrusion Process

Extrusion can be defined as the process of subjecting a material to compression so that it is forced to flow through a confined suitably shaped opening called the die. The metal is forced through the die and the cross-section of the die determines the shape properties of the resulting product. Extrusion may be done either on cold metal or on heated metal. One of the analogies that can be offered to the process of extrusion is that of squeezing a tube of toothpaste. The metal billet is placed in the billet chamber and is forced by the ram through a die.

Extrusion is one of the best amongst all metal forming processes; advantages of metal forming process:

- (i) Saving in material due to less wastage

- (ii) Strength is increased due to cold work and better grain flow.
- (iii) Corrosion and wear resistance are improved
- (iv) Fatigue properties are improved
- (v) Better tolerances in geometry and size of the product
- (vi) Production rates are increased.

In recent years, owing to the development of numerical methods of analysis, more detailed information can be obtained from the computation. Numerical solutions have been proposed for axisymmetric and plane strain extrusion problems.

In this journal, authors search few selected research papers related to Extrusion process using Upper -Bound Method and Finite Element Analysis Method.

1.2 Upper Bound Method

Sahoo et al. [1] reformulated the SERR technique so that it can be used for analyzing extrusion of round billets. The circular cross-section of the round billet is approximated by a regular polygon of equal area and the number of sides of the polygon is increased progressively until convergence of the extrusion pressure is achieved. As a test, the extrusion of hexagon-section bars from round billets through linearly converging dies was analyzed. It can also be used for other section's billets like channel section, triangular section, square section etc.

Sahoo et al. [2] presented an upper-bound analysis for the extrusion of bars of channel section from square/rectangular billets through rough square dies. A class of kinematically admissible discontinuous velocity fields, based on the reformulated SERR technique, is examined and the velocity field giving the lowest upper-bound is identified. This velocity fields is used to compute the upper-bound extrusion pressure for various area reduction

Maity et al. [3] proposed an upper-bound analysis for the extrusion of square sections from square billets through curved dies having prescribed profiles. They derived kinematically-admissible velocity fields using dual-stream-function technique. They present analytical results for both sticking friction and frictionless condition. For sticking friction condition they optimize the die geometry with respect to appropriate parameters. They found that in case of cosine die extrusion pressure is low in frictionless condition because entry and exit angle is zero. Under sticking-friction conditions the best upper-bound is provided by a straight tapered die.

Narayanasamy et al. [4] proposed streamlined extrusion dies by modifying the conventional extrusion dies to incorporate gradual reduction in the area of cross-section in order to ensure smooth flow of metal and to dispense with the problems faced by the conventional dies such as formation of dead metal zone, non-uniform flow of metal, more redundant work etc. The profile of the streamlined extrusion dies is the crucial parameter to optimize the extrusion process. Many profiles such as third order polynomial equation, fifth order polynomial equation, Bezier curve, etc., have been suggested for the design of streamlined extrusion dies with the view to reduce the extrusion load for the given reduction ratio. They suggested extrusion dies with cosine profile to extrude circular billet to circular shape and using upper bound solution plastic deformation work required for extrusion is determined. It has been proved that the die designed based on cosine profile is superior to the conventional shear dies and the straightly converging dies.

Frisch and Mata-Pietric [5] investigated upper bound solution of axisymmetric components through cosine, elliptical and hyperbolic die profiles and validated experiments with good agreements.

Altan et al. [6] analysed the deformation of the material during a 90° equal-channel angular extrusion (ECAE) process using upper-bound theorem. The model suggested includes the effect of friction between

the sample and the die walls, radius of inner corner of the die and the dead metal zone on the deformation patterns during ECAE. The parameters of the model are explored in relation to the deformation of the material during the process. Further directions for progress in deformation analysis in severe plastic deformation processes are outlined.

Ajiboye et al. [7] studied the effect of die land length on the extrusion pressure. They found that extrusion pressure increases with increasing in complexity of die geometry; for particular reduction and die length, the extrusion pressure is highest for rectangular section and lowest for square section. They found that for a particular reduction in area extrusion pressure increases with increasing die land length and vice-versa.

Paydara et al. [8] analyzed the equal channel angular extrusion with circular cross-sections using upper-bound analysis, and the power dissipated on all frictional and velocity discontinuity surfaces are determined and the total power optimized analytically. The theoretical results is compared with experiments, and it is found that the size of the plastic deformation zone and the relative extrusion pressure increase with increasing the constant friction factor. In addition the results show that there is a good agreement between the theoretical and experimental load displacement curve.

Kim et.al [9] derived the generalized velocity field for three-dimensional square-die forward extrusion of circular-shaped bars using billets of regular polygon. They determine the upper-bound extrusion load; the velocity distribution and the average length of the extruded billets by minimizing the total power consumption with respect to chosen parameters by the proposed simple kinematically-admissible velocity field. It is found that the theoretical predictions and experimental results of the extrusion load and the average extruded length are in good agreement.

Sahoo [10] studies some experimental result of extrusion of hexagon, channel, triangle and cross sections using square dies and compare with theoretical result (using SERR technique)

Kim et al. [11] calculated the powers required in the steady-state CONFORM process. For this, similarity is applied to the CONFORM process for an equivalent side extrusion process, to which the upper bound method is used to derive the equation for calculating the powers. Even though the global flow characteristics between the real and the simplified processes are not similar, the calculated results for both processes show good agreement. And FEM simulation were carried out using the DEFORM software in order to verify the theoretical results.

Gordon et.al [12] used the adaptable die design method, in conjunction with an upper bound method that allows the rapid evaluation of a large number of die shapes and the discovery of the one that produces the desired outcome. A double optimization process is used to determine the values for the flexible variables in the velocity field and secondly to determine the die shape that best meets the given criteria.

Venkata Reddy et al. [13] presented the optimal design of axisymmetric dies using upper-bound method and finite-element method (FEM). They modeled billet material during plastic deformation process as visco-plastic rate sensitive material and flow stress to be strain rate and temperature dependent. They observed that the optimal die length decreases with friction factor and increases with reduction ratio and ram velocity. The extrusion power required is lowest for the stream-lined die with cosine die following closely behind. However hyperbolic dies are better than the conical die at lower reduction ratios, whilst the conical die is superior at greater reduction ratios.

Sinha et al. [14] described the procedure for the design of a multi-hole extrusion process. For the same sizes of the holes, the ram force in a single-hole extrusion process is more than in a multi-hole extrusion

process. Therefore, a simplified upper bound and slab method analysis has been carried out for a single-hole extrusion process. The ram and die pressures obtained from this analysis are used for designing a multi-hole extrusion process setup. The stresses in the die are computed using the finite element method. Based on this approach, an experimental setup was fabricated and experimental study was carried out.

Johnson [15] investigated the effects of section shape and punch speed on the necessary extrusion load, and the nature of the flow of metal within the extruded rod for extrusion of pure lead and tellurium lead rods of circular, square, rectangular, triangular and I section. It is shown that, for a given reduction in area, the load is independent of section shape for all but re-entrant shapes and increases with increase in extrusion speed.

Maity et al. [16] studied the effect of mathematically contoured die on surface integrity of extruded product. They used three dimensional upper bound methods using dual stream function method to obtain non-dimensional extrusion pressure and optimum die length for cosine die profile for different reductions. They found that the experimental results are compatible with the theory.

Basily and Sansome [17] calculated the maximum reduction of area obtainable for drawing section from a lower bound analysis they found that this reduction is less than when drawing round rod from round bar. They presented a lower bound solution in detail and compared the upper bound solution and found that, not only the draw stress can be calculated but the equivalent die angle can be optimized for every relevant combination of the coefficient of friction and percentage reduction in area.

Nagpal and Altan [18] introduced the concept of dual stream functions to express three dimensional metal flows in the dies and analyzed the force of extrusion from round billet to elliptical bars.

Yang and Lee [19] proposed a new method of analysis for the extrusion of arbitrarily shaped sections through curved die profiles. They found a kinematically admissible velocity field by deriving the equation of a stream line. To determine the extrusion pressure for the rigid-perfectly plastic material upper-bound method is then applied. They obtained general formulation for an arbitrary cross section using conformal transformation. They discussed the effects of sectional shape, die profile and interfacial friction at the die surface.

Prakash and Khan [20] suggested a generalized expression for the spherical flow field generated by plastic flow of metal through a converging die of regular polygonal cross-section. They suggested that the expression is valid for all the possible boundary shapes of the zone of plastic deformation. They calculated the working stress for a rigid-perfectly plastic material by applying upper-bound techniques assuming that the boundaries of the zone of plastic deformation are exponential cylindrical surfaces. A constant frictional stress is assumed to be acting over the entire die-material interface. The working stress relation is minimized with respect to the shape of the boundaries of deformation zone, thus yielding a better upper-bound value of the working stress compared to the working stress for cylindrical boundaries. The effects of various process parameters on the working stress and the shape of the zone of deformation are given in graphical form. The analysis predicts optimum, dead zone and critical angles. Comparisons with earlier theories have been made and it is concluded that the theory presented is a more generalized theory and yields better results for large die angles.

Gatto and Giarda [21] analyzed three-dimensional kinematic model by limit analysis for plastic deformation, denoted as SERR (Spatial Elementary Rigid Regions), in more detail. They found that the characteristics of some spatial figures, which are considered as particularly useful in partitioning the plastic volume in the limit

analysis of the three-dimensional cases are given, together with some simple applications of the methods to practical cases of extrusion.

1.3. Finite element analysis

Halvorsen and Aukrust [22] studied the buckling or waving of extruded flat sections using Lagrangian FEM software, MSC Super Form.

They performed some extrusion experiments to verify both the simulations and the mechanisms observed in the FEM simulations.

Lof and Blokhuis [23] presented a method for the simulation of the extrusion of complex profiles, which can be used in an industrial environment. They modeled bearing area with an equivalent bearing model to describe the resistance in the bearing without using a large number of elements. They developed a specialized pre-processor to avoid the time-consuming and complex work necessary for the development of the FEM model for a particular die.

Gang et al. [24] performed a 3D computer simulations to determine the effects of the ram speed and the billet temperature on the extrusion temperature and the peak extrusion pressure. The ram speed and the billet temperature are the primary process variables that determine the quality of the extruded magnesium profile and the productivity of the extrusion operation. The optimization of the extrusion process concerns the interplay between these two variables in relation to the extrudate temperature and the peak extrusion pressure. The 3D computer simulations were performed to determine the effects of the ram speed and the billet temperature on the extrudate temperature and the peak extrusion pressure, thereby providing guidelines for the process optimization and minimizing the number of trial extrusion runs needed for the process optimization. A case study on the extrusion of an AZ31 X-shaped profile was conducted. The correlations between the process variables and the response from the deformed material, extrudate temperature and peak extrusion pressure were established from the 3D FEM simulations and verified by the experiment. The research opens up a way to rational selection of the process variables for ensured quality and maximum productivity of the magnesium extrusion.

Chanda et al. [25] investigated the effect of process parameter namely iso-speed and step wise ram speed on extrusion pressure the thermal response of the work piece and stress state of round bar using computer simulation. They found that step wise ram speed decrease enables the temperature to reach steady state which corresponds to nearly constant exit temperature.

Chanda et al. [26] performed the 3D FEM simulation of extrusion of aluminium to determine the state of stress, strain and the temperature of a commercial aluminium alloy going through square and round dies. They found that at the same process conditions, the state of stress in the aluminium alloy going through a round die is more favourable than going through a square die, especially at a high reduction ratio. The magnitude of the tensile stress component at the corners of the square extrudate is much higher than at the surface of the round extrudate, which makes the square extrudate more tearing prone. Simulation also reveals that while temperature evolution during the process is similar for both of the die shapes, temperature rise across the section is prominent, especially at sharp corners of the square extrudate. The magnitude of the tensile stress component at the corners of the square extrudate is much higher than at the surface of the round extrudate, which makes the square extrudate more tearing prone.

Hu et al. [27] developed a thermo-mechanically coupled elasto-plastic FEM system based on ANSYS software and the finite strain theory. They simulated the deep warm extrusion of a thin-walled cup. The basic parameters for process development and die design such as

the metal flow, and the distribution of stresses, strains and temperature in the die and the workpiece, taking into account conduction, convection, radiation and plastic work, the loading-time curve, and the cause of failure on the punch, are obtained and analyzed. They found that simulation result agree with experimental results.

Bouzakis et al. [28] simulated the flow of wet ground clay ram extrusion device and by a FEM-based model, considering the von Mises criterion for the flow stress, the associative flow rule and the rigid-viscoplastic constitutive equation. The friction between clay and die is approached by the Tresca boundary condition, which proves a more realistic approach than the Coulomb friction law for the contact conditions between a plastically deforming material and a rigid surface. It is found that no sticking areas appear on the mandrel surface.

Li et al. [29] presented a results from a series of pocket designs that were modelled using finite element method (FEM) to systematically investigate the influence of the pocket design parameters on the metal flow In extrusion die design, it has become increasingly common to use „pocket“ technology to balance the metal flow. They studied the effects of pocket angle and size on metal flow and it is shown that pocket angle plays an important role influencing metal flow velocity, whilst pocket volume has much less effect on velocity.

Peng et al. [30] used the commercial FEM code FORGE3 to study the influence of the number and the distribution of die holes on extrusion parameters. The flow pattern, pressure requirements, and temperature histories developed are established and it is clearly shown by the FEM simulations that agreement with experimental results is obtained. They obtained metallurgical behavior (the substructure, recrystallised grain size and the fraction recrystallised) from these simulations. They compared the results with extrusion through a single-hole die

Fang et al. [31] investigate the effect of steps in the die pocket on metal flow to produce two chevron profiles with unequal thicknesses through two-hole dies, by means of 3D FEM simulation of extrusion in the transient state. They found that the pocket step could be effectively used to balance metal flow. They demonstrate the 3D FEM to be a powerful tool in optimizing die design and decreasing the number of trial extrusion runs.

Duana et al. [32] explored the complicated interactions between die design, forming parameters (i.e. ram speed, container temperature, billet temperature and extrusion ratio) and the product qualities (extrudate shape, surface condition and microstructure) by the use of finite element modeling (FEM). The various models (such as recrystallization, damage criteria, etc.) have been integrated into the commercial codes, FORGE2 and FORGE3, through user routines. They found that the use of an expansion chamber can significantly reduce the degree of non-uniformity in terms of the extruded product shape and properties. The character of the complex material flow is also identifiable, which is very useful to help improve die design.

Lee et al. [33] studied the effect of bearing lengths for the control of material flow in the die in hot extrusion. They used the three-dimensional non-steady analysis using the thermo-rigid-viscoplastic element method that includes an automatic remeshing module. It was found that the design equation determined bearing lengths that resulted in a fairly uniform exit velocity distribution throughout the extruded section. From the results of this study, it was found that the proposed design equation can be effectively used to estimate appropriate bearing lengths.

2.0 MATERIALS, METHODS AND MODEL DEVELOPMENT

Many extrusion parameters have been looked into by many researchers in the past as reviewed in this chapter. In the present work, the authors:

- use Finite element simulations to study the process of axisymmetric extrusion process using Aluminum alloy
- AA6063 in order to increase the understanding of the process,
- designed mathematically contoured curved die profiles for extrusion of circular, square, triangular, hexagonal, heptagonal and octagonal sections from round billet.
- carried out a numerical analysis using DEFORM software for extrusion of the above sections from round billet
- determined the extrusion load with respect to ram travel both for dry and lubricated condition
- predicted the effective stress, strain rate, strains and temperature distribution in the deformation zone
- determined the extrusion pressure with respect to reductions for different frictional boundary conditions.

2.1 Die design profile

In the present investigation the curved die profiles have been designed for extrusion of circular, square, triangular, hexagonal, heptagonal and octagonal section from round billet. First of all a mathematical equation of the die profile is derived. Then using MATLAB R2009b we calculate the co-ordinate of the die profile. A solid CAD model for the curved die profile is made using Autodesk Inventor 2013 software

2.2 Geometry of die profile for extrusion of circular section from round billet.

The billet is of circular shape with radius R , r = radius of the circular section at the exit. If the percentage fraction of reduction is $(1 - Q)$, then

$$\frac{\pi R^2 - \pi r^2}{\pi R^2} = (1 - Q) \quad (1)$$

From where the exit (product) radius is obtained to be

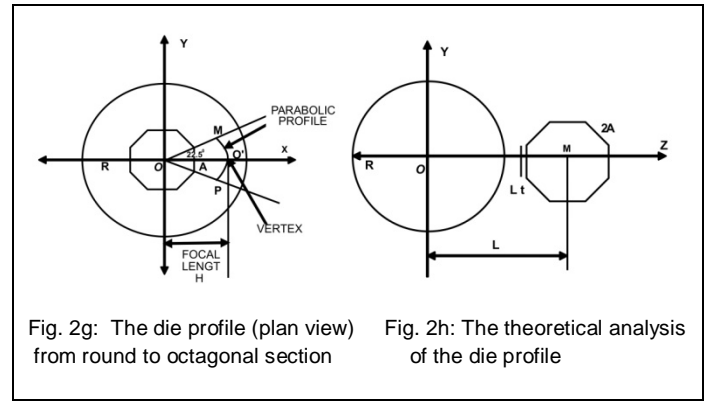
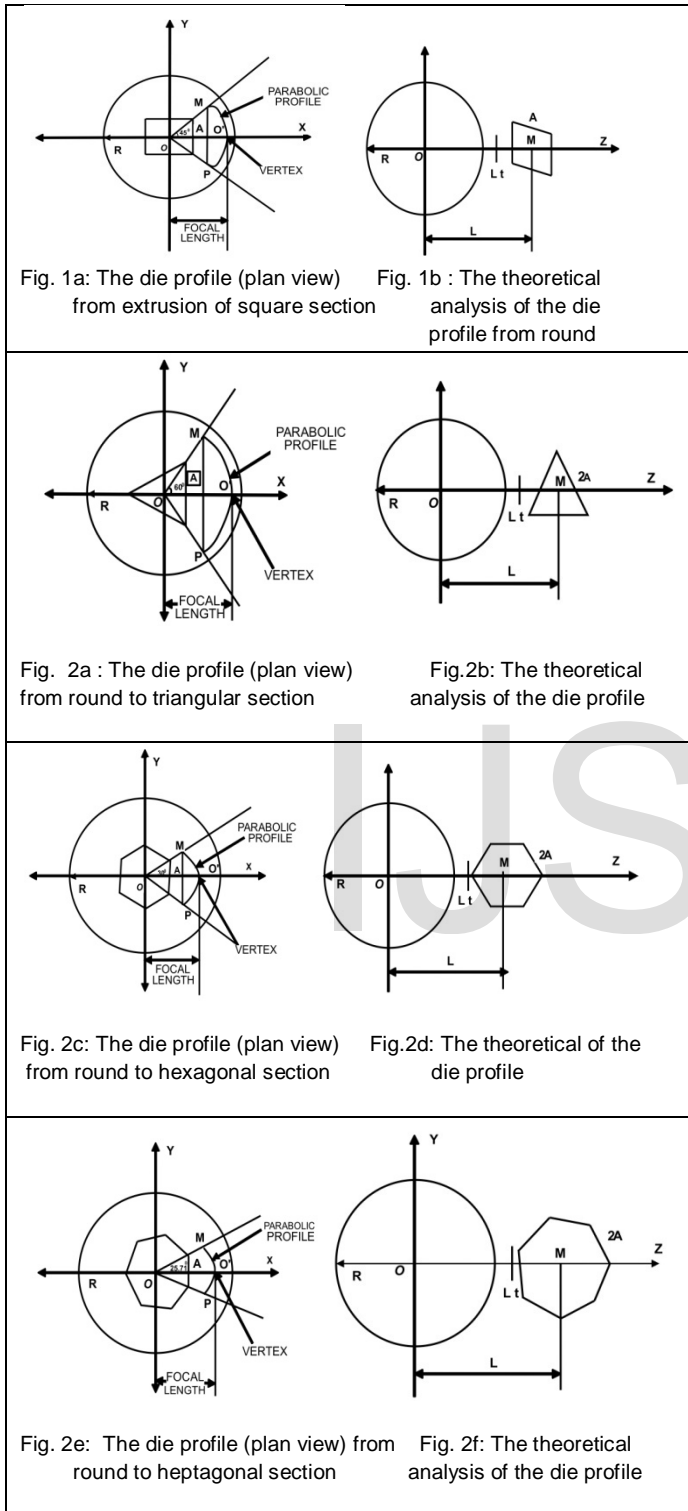
$$r = \sqrt{R^2 Q} \quad \text{or} \quad r = R\sqrt{Q} \quad (2)$$

2.3 Design of streamlined extrusion dies for extrusion of square section with curved die profile.

The die profile is designed in such a manner so that the square section is converted gradually from round billet (see figures 1a and 1b for square geometry, also figure 2a to 2h defined different geometrical shapes). In order to achieve this, a parabolic function has been considered. The billet is of circular shape with radius R and the product is of square shape with half width A . Half diagonal of the square is $\sqrt{2}A$.

Let N be the total number steps required for conversion of round shape to square shape and P be the number of any intermediate steps.

Table 1: Design of Streamlined extrusion dies for extrusion of different sections with curved die profile



After 'P' steps, the die section is a parabolic profile POM as shown in Figure 1

$$\text{Focal length} = a = OO' = R - (R - A) \frac{P}{A}$$

$$\text{Length } (OM) = OP = R - (R - \sqrt{2}A) \frac{P}{N}$$

x and y co-ordinates are same for the above length. $x = y = OM \cos 45^\circ = OM \sin 45^\circ$

The general equation of the parabola can be derived using three points on it as follows:

$$-y^2 = 4\alpha(x - a) \quad (3)$$

In the above equation, the parabola has focus point at (-a, 0) and axis along x-axis.

The parabola is open to the right of y-axis.

To determine 4α , we proceeded as follows. The parabola MO'P passes through the points $(x, \pm y)$

$$\left\{ \left[R - (R\sqrt{2}A) \left(\frac{P}{N} \right) \right] \frac{1}{\sqrt{2}A}, \pm \left[R - (R - \sqrt{2}A) \left(\frac{P}{N} \right) \right] \frac{1}{\sqrt{2}} \right\} \quad (4)$$

Substituting the value of focal length 'a' in equation (2), the parabolic equation is given by

$$-y^2 = 4\alpha \left\{ x - \left[R - (R - A) \left(\frac{P}{N} \right) \right] \right\} \quad (5)$$

Using (4) in (5), we have

$$4\alpha = \frac{\left(\frac{1}{2} \right) \left[R \left(1 - \frac{P}{N} \right) + \left(\frac{1}{\sqrt{2}} \right) \left(\frac{P}{N} \right) \right]}{\left\{ R \left(1 - \frac{P}{N} \right) \left(1 - \frac{P}{N} \right) \right\}} \quad (6)$$

Substituting for 4α in (5) we have

$$y^2 = \frac{\left(\frac{1}{2} \right) \left[R \left(1 - \frac{P}{N} \right) + \sqrt{2}A \left(\frac{P}{N} \right) \right]}{\left\{ R \left(1 - \frac{P}{N} \right) \left(1 - \frac{P}{N} \right) \right\}} \left[\left(R - (R - A) \left(\frac{P}{N} \right) - x \right) \right] \quad (7)$$

From equation (7), we will get the different parabola surfaces by Putting

$P = 1, 2, 3, \dots, N-1$

Considering the die profile at different depths with parameter $(t = \frac{P}{N})$ where the total die depth is assumed to be L. When $t=0, Z=0$ this is corresponding to the entrance plane of die and $t=1, Z=L$ at the exit plane, where L is the die length. Similar to the round to circular, if the percentage fraction of reduction is $(1 - Q)$, then

$\frac{\pi R^2 - 4A^2}{\pi R^2} = (1 - Q)$. From where, $2A = R(\sqrt{\pi Q})$ and semi diagonal length is

$$A \times \sqrt{2} = \frac{R}{2} (\sqrt{\pi Q}) \sqrt{2} = \frac{R}{\sqrt{2}} (\sqrt{\pi Q})$$

For any value of t, if $y=0$, then, the x co-ordinate of O' is

$$R \left(1 - t + t \sqrt{\frac{\pi Q}{4}} \right), \text{ Where } t = \frac{P}{N} \text{ and}$$

The y co-ordinate of O' is = 0
 The x co-ordinate of M and P is

$$\left[\frac{R}{\sqrt{2}} \left(1 - t + t \sqrt{\pi \frac{Q}{2}} \right) \right]$$

while the y-coordinate of M is

$$\left[\frac{R}{\sqrt{2}} \left(1 - t + t \sqrt{\pi \frac{P}{2}} \right) \right] \text{ and } \left[\frac{R}{\sqrt{2}} \left(1 - t + t \sqrt{\pi \frac{Q}{2}} \right) \right], \text{ respectively. The}$$

equation of the parabola is

$$y^2 = 4\alpha \left[\left(R \left\{ 1 - t + t \sqrt{\pi \frac{Q}{4}} \right\} - x \right) \right] \quad (8)$$

From where substituting the values of x and y as given above, α is determined as

$$4\alpha = \frac{R \left(1 - t + t \sqrt{\pi \frac{Q}{2}} \right)}{\left[2 \left(1 - \frac{1}{\sqrt{2}} \right) (1 - t) \right]} \quad (9)$$

Using (9) in (8), we have

$$y^2 = \frac{R \left(1 - t + t \sqrt{\pi \frac{Q}{2}} \right)}{\left[2 \left(1 - \frac{1}{\sqrt{2}} \right) (1 - t) \right]} \left(R \left(1 - t + t \sqrt{\pi \frac{Q}{4}} \right) - x \right) \quad (10)$$

Here t represents a depth parameter and the equation (10) gives the equation of the surface. This equation is called parametric equation where $t = \frac{Z}{L}$, which then becomes the equation of the profile,

In a similar manner, the profiles of all the shapes considered were derived and tabulated as shown in **table 2** below.

2.4 Geometry of die profile for extrusion of T, L and H-section from round billet.

Figure 3-5 show the die profile (plan view) from round to T, L and H-section respectively. For L and T-section, If the percentage fraction of reduction is $(1 - Q)$, then,

$\frac{\pi R^2 - 5l^2}{\pi R^2} = (1 - Q)$ [5l² is the area of the square T and L-section], from where $\pi R^2 - 5l^2 = \pi R^2(1 - Q)$. The length l, thickness of the square L and T-section is $l = R \sqrt{\frac{\pi Q}{5}}$

For H-section, the percentage fraction of reduction is $(1 - Q)$, then $\frac{\pi R^2 - 7l^2}{\pi R^2} = (1 - Q)$ [7l² is the area of the square H-section], from where $\pi R^2 - 7l^2 = \pi R^2(1 - Q)$. The length l, thickness of the square H-section is $l = R \sqrt{\frac{\pi Q}{7}}$

2.5 Solid model

MATLAB R2009b was used to generate the number of points using above generated die profile equation. The generated points were used to create solid model using Autodesk inventor 2013. Solid model generated from Autodesk inventor 2013 were show in the following figures 6-11.

FEM modeling has been carried out using 3D deform software. A solid CAD model for the curved die profile is made using Autodesk Inventor. Cad model for extrusion of non- axisymmetric sections (L, T and H) from round billet are given in figure 12-14. The length of die is taken as 40mm. the solid CAD models are developed for 50% reduction.

Table 2: Parametric Equation representing profile of different Shapes

Geometry	Parametric equation	x
Square	$y^2 = \frac{R \left(1 - t + t \sqrt{\pi \frac{Q}{2}} \right)}{\left(2 \left(1 - \frac{1}{\sqrt{2}} \right) (1 - t) \right)} \left(R \left(1 - t + t \sqrt{\pi \frac{Q}{4}} \right) - x \right)$	$x = \left(\frac{R}{2} \right) \sqrt{\pi Q}$
Triangle	$y^2 = \frac{3R \left(1 - t + \frac{2t}{3} \sqrt{\pi Q} \right)^2}{4 \left(\frac{1}{2} - \frac{t}{2} - \frac{t}{3} \sqrt{\pi Q} \right)} \left(R \left(1 - t + \frac{t}{3} \sqrt{\pi Q} \right) - x \right)$	$x = \frac{2}{\sqrt{3}} R \sqrt{\left(\frac{\pi Q}{3} \right)}$
Hexagonal	$y^2 = \frac{R \left(1 - t + 0.62t \sqrt{\pi Q} \right)^2}{(0.536(1 - t))} \left(R \left(1 - t + 0.31t \sqrt{\pi Q} \right) - x \right)$	$x = 0.62 \sqrt{\pi Q}$
Heptagonal	$y^2 = \frac{0.188R \left(1 - t + 0.604t \sqrt{\pi Q} \right)^2}{(0.099(1 - t))} \left(R \left(1 - t + 0.31t \sqrt{\pi Q} \right) - x \right)$	$x = 0.604 \sqrt{\pi Q}$
Octagonal	$y^2 = 4\alpha = \frac{0.854R \left(1 - t + 0.595t \sqrt{\pi Q} \right)^2}{(0.076(1 - t))} \left(R \left(1 - t + 0.298t \sqrt{\pi Q} \right) - x \right)$	$x = 0.604 \sqrt{\pi Q}$

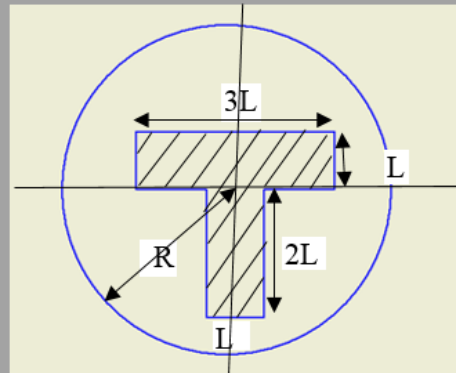


Fig. 3. The die profile (plan view) from round to T-section

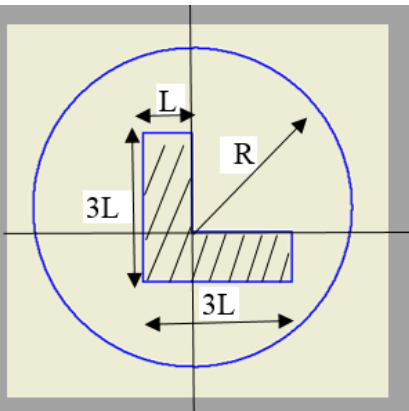


Fig. 4. The die profile (plan view) from round to L-section

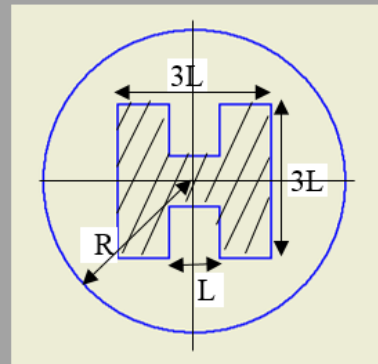


Fig. 5. The die profile (plan view) from round to H-section



Fig. 6. Streamlined die for extrusion of circular section

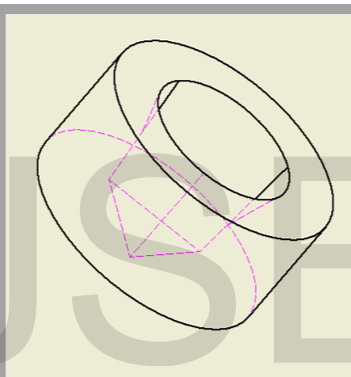


Fig. 7. Streamlined die for extrusion of triangular section

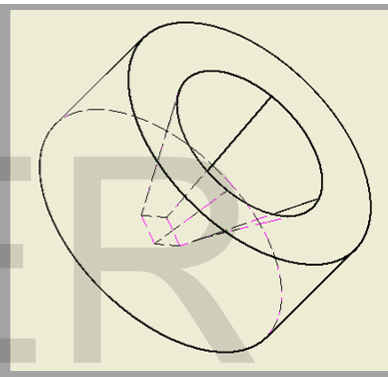


Fig. 8. Streamlined die for extrusion of square section

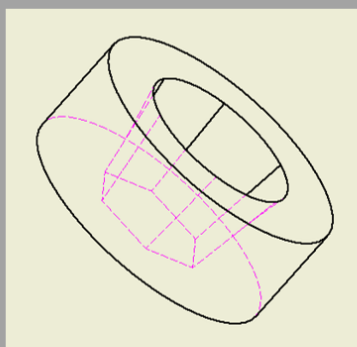


Fig. 9. Streamlined die for extrusion of hexagonal section

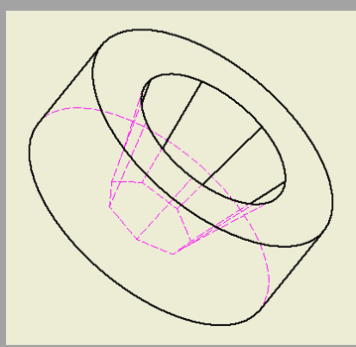


Fig. 10. Streamlined die for extrusion of heptagonal section



Fig. 11. Streamlined die for extrusion of octagonal section

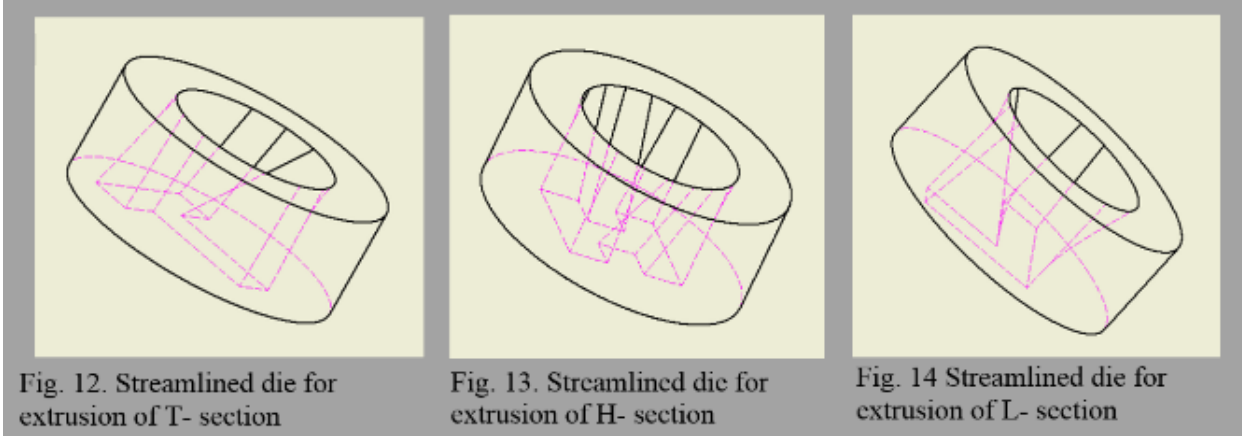


Fig. 12. Streamlined die for extrusion of T- section

Fig. 13. Streamlined die for extrusion of H- section

Fig. 14 Streamlined die for extrusion of L- section

2.7 FEM simulation

The actual FEM-based analysis is carried out in this portion of DEFORM-3D.

This simulation engine is based on a rigid-plastic FE formulation and can handle a multiple number of billets and dies with non-isothermal simulation capability. This is the programme which actually performs the numerical calculations for solution of the problem [34]. In the present investigation, round billet of rigid plastic material for extrusion of triangular, square, hexagonal, heptagonal and octagonal section is modeled with a rigid curved die.

The tetrahedral solid elements are taken for analysis. The work-material is taken as Aluminum AA6063, which is plastic in nature. The mesh is generated automatically in the model as shown in Fig. 15

2.6 MATERIAL COMPOSITION

The constant friction factor is assumed in the modeling. The modeling has been carried out both for dry and lubricated condition. The values of 'm' are 0.38 and 0.75 for wet and dry conditions respectively. The operation has been carried out at room temperature.

The table shows the parameter input for the simulation and Details of individual component

Table 3: Parameters Used In Simulation

Parameters	Temperature	Strain Rate	Ram Speed	Friction Factor 'm'
Inputs	30 ⁰	0.25s ⁻¹	0.075mm/s	0.38 & 0.75

Table 4: Details of individual component for simulation set-up

S/n	Name of Parts	Dimension of Part (mm)		Materials
		Cross Section	Length	
1	Billet	Φ60	80	Aluminum alloy 6063,
2	Punch	Φ60	120	Rigid
3	Bottom die with Opening	Φ100 external Φ60 internal	40 - 50	Rigid
4	Ram	Φ100 external Φ60 internal	100	Rigid

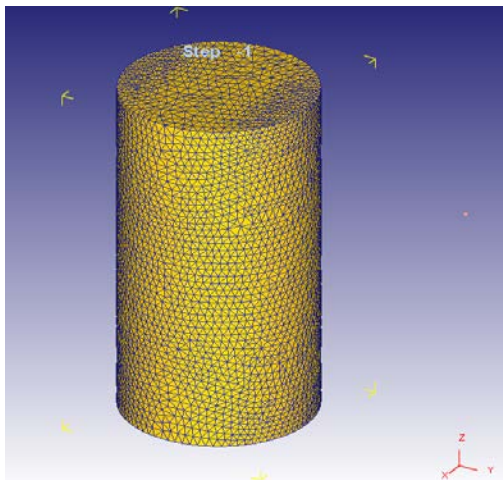


Fig. 15: Mess formulation (tetrahedral) for square billet (SizeRatio=1; Number of elements =50000)

2.8 Properties and composition of workpiece/billets

Aluminum alloy AA6063 properties and composition is a shown in the table below

Table 5: AA6063 Composition And Properties
 (Ref: Online Material Data Base Efundu)

Element	Weight %
Al	98.9
Si	0.40
Mg	0.70

THERMAL PROPERTIES	
Thermal Expansion ($10^{-6}/^{\circ}\text{C}$)	23.4
Thermal Conductivity (w/m-k)	218

Table 6: AA6063 Composition and Properties
 (Ref: Online Material Data Base Efundu).

MECHANICAL PROPERTIES	
Density ($\times 1000\text{kg}/\text{m}^3$)	2.7
Poisson's Ratio	0.33
Elastic Modulus (GPa)	70 – 80
Tensile Strength (MPa)	90
Yield Strength (MPa)	48
Hardness (HB500)	25
Shear Strength (MPa)	69
Fatigue Strength (MPa)	55

3.0 RESULT AND DISCUSSION

3.1 Extrusion load and punch displacement

The load prediction versus punch travel during the extrusion of circular, triangular, square, hexagonal, heptagonal and octagonal-cross section from round billet for 90% reduction for lubricated condition ($m=0.38$), are shown in figures 16-21, respectively. The extrusion load as it is felt by all the components, such as the billet, container, bottom die and the punch, involved is shown below. Notice that in all the graphs, the billet resists load least, follow by the container and then the bottom die while the punch felt the load most during the operation. Also, while the wavy behaviour was rather more pronounced with the container and the punch, it's almost not seen as in the billet deformation as well as in the bottom die. This wavy behaviour is probably due to the initial filling of the die by the billet as it is seen to be more pronounced as the complexity of the die increases. This wavy observation is likely to impact on the live span of the tool. A comparison of extrusion loads versus punch displacements or stroke curves for the aluminium alloy AA6063 is shown in figure 22 for extrusion of axisymmetric (circular, triangular, square, hexagonal, heptagonal and octagonal) shaped sections and asymmetric (L, T and H) cross section from round billet through curve dies for 50% reduction at room temperature. While there is no marked difference between the predictive loads for symmetric shapes, the L-section has the highest extrusion load, followed by T-section and H-section given the least pressure for asymmetric

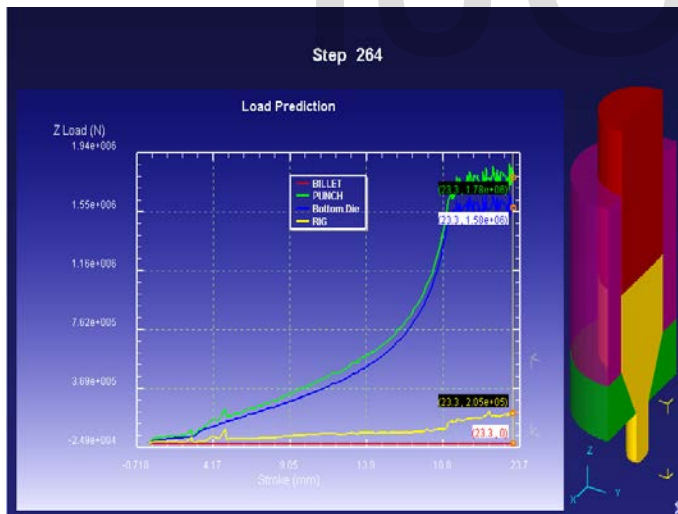


Fig. 16: Variation of punch load with respect to punch travel for extrusion of circular section (90% reduction)

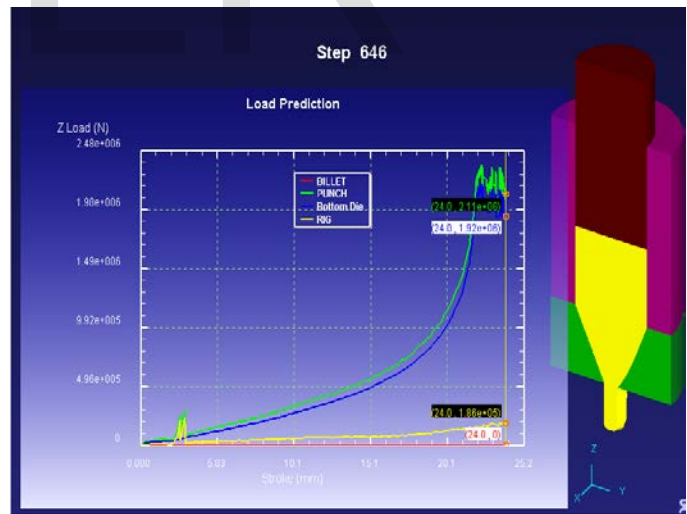


Fig. 17: Variation of punch load with respect to punch travel for extrusion of triangular section (90% reduction)

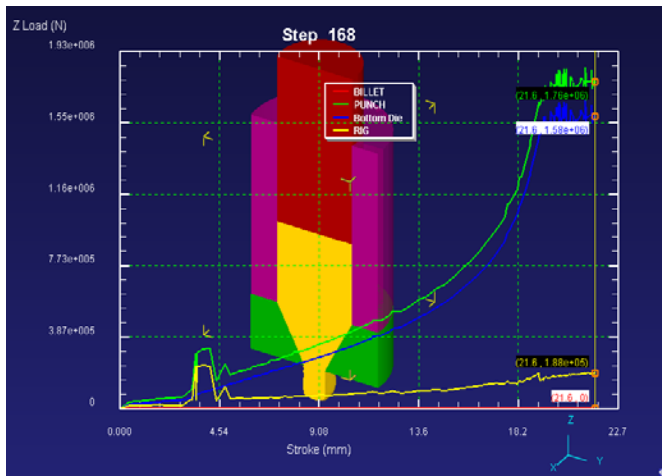


Fig. 18: Variation of punch load with respect to punch travel for extrusion of square section $m=0.38$ (90% reduction)

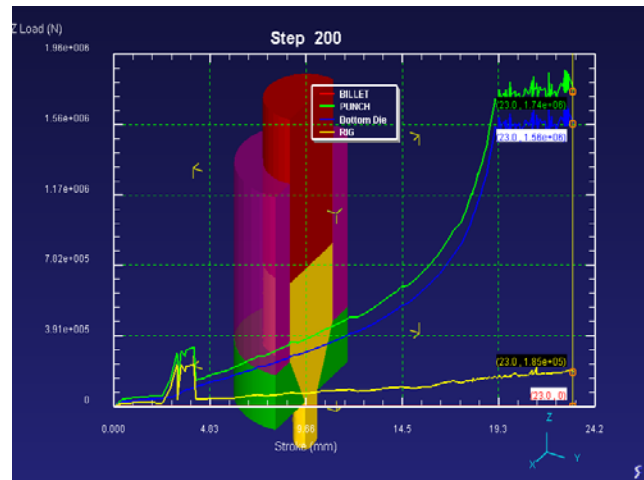


Fig. 19: Variation of punch load with respect to punch travel for extrusion of hexagonal section $m=0.38$ (90% reduction)

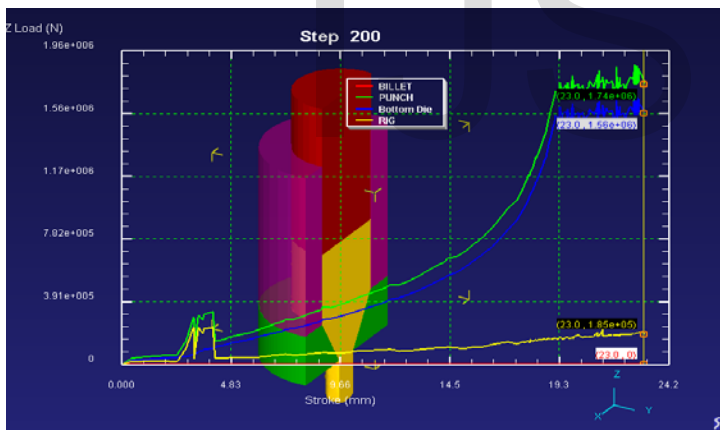


Fig. 20: Variation of punch load with respect to punch travel for extrusion of heptagonal section $m=0.38$ (90% reduction)

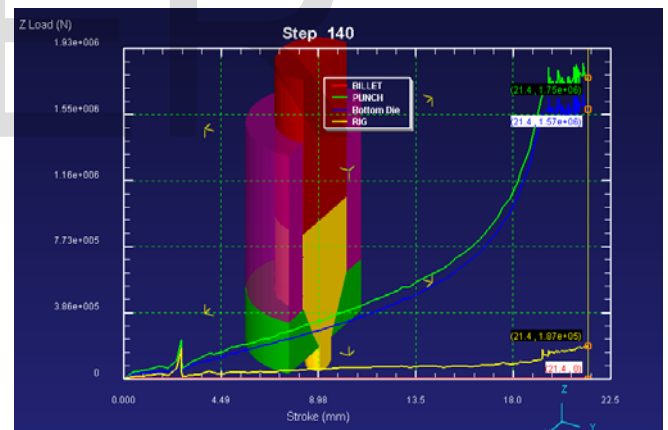


Fig. 21: Variation of punch load with respect to punch travel for extrusion of section $m=0.38$ (90% reduction)

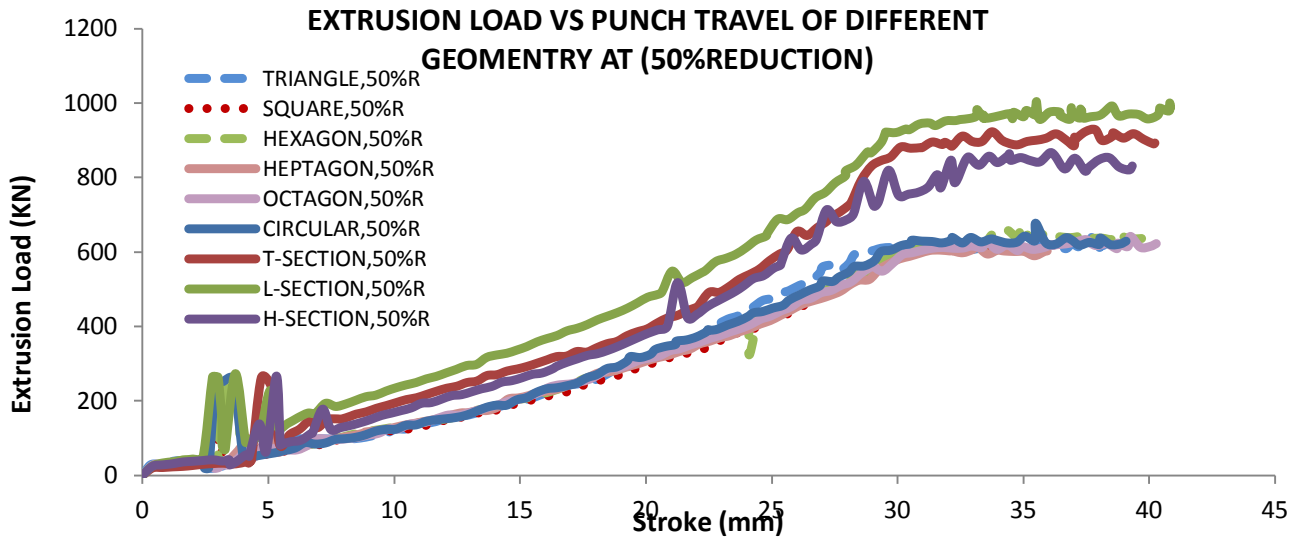


Fig. 22 : Comparison of extrusion load versus punch travel for axisymmetric and asymmetric

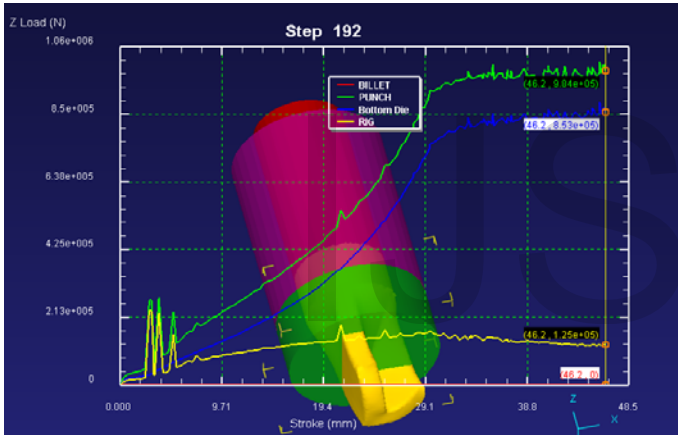


Fig. 23: Variation of punch load with respect to punch travel for extrusion of L- section $m=0.38$ (50%)

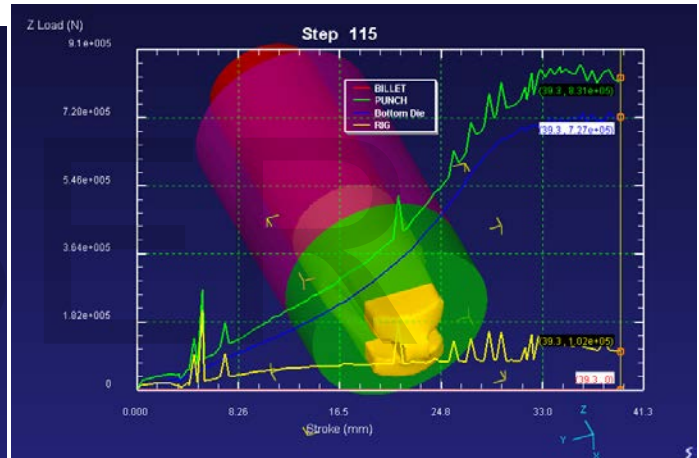


Fig. 24: Variation of punch load with respect punch travel for H- section $m=0.38$ (50% reduction)

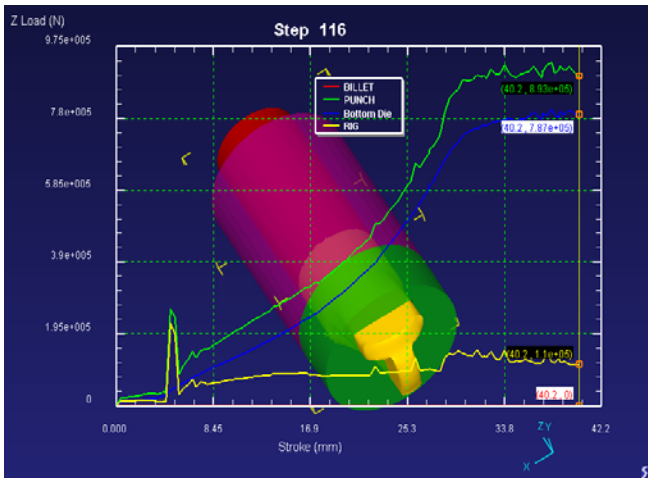


Fig. 25: Variation of punch load with respect to punch travel for extrusion of T- section $m=0.38$ (50% reduction)

Table 7: Maximum dimensionless extrusion pressure of various geometry and at indicated percentage area reductions

GEOMETRY	Wet (m=0.38) $\frac{P}{\sigma_0}$				Dry (m=0.75) $\frac{P}{\sigma_0}$		
	R=50%	R=50% Exper.	R=70%	R=90%	R=50%	R=70%	R=90%
Triangle	1.68		2.37	4.06	2.68	3.86	5.55
Square	1.51	1.48[16]	2.18	3.88	2.66	3.68	5.38
hexagonal	1.39		2.12	3.83	2.45	3.43	5.04
Heptagonal	1.30		2.12	3.83	2.43	3.40	5.11
octagonal	1.28		2.01	3.81	2.43	3.45	5.14
circular	1.31		2.12	3.70	2.11	3.39	5.06
H-section	1.80						
T-section	1.92						
L-section	2.03						

Table 7 shows the maximum dimensionless extrusion pressure of various geometries at indicated percentage area reductions. Generally, it can be observed that as the side of the considered polygons increases, the extrusion pressure decreases for both wet and dry conditions at the indicated percentage area reductions. This is probably due to the ease of the metal flow as the shape of exit geometry is approaching the shape of entry geometry and moreover the die cross section is designed to gradually reduce from circular to the exit polygon. The maximum temperature generated also follows the same pattern with triangular given the highest temperature, followed by square while the remaining geometries, such as hexagonal, heptagonal, octagonal and circular virtually maintained the same temperature.

The load prediction versus punch travel are shown in Fig. 23-25 for extrusion of L, H and T section from round billet for 50% reduction for lubricated condition (m=0.38), respectively. The extrusion load as it is felt by all the components, such as the billet, container, bottom die and the punch, involved is shown on each figure. Notice that in all the three graphs, the billet resists load least, follow by the container and then the bottom die while the punch felt the load most during the operation. Also, while the wavy behaviour was rather more pronounced with the container and the punch, it's almost not seen as in the billet deformation as well as in the bottom die. This wavy behaviour is probably due to the initial filling of the die by the billet as it is seen to be more pronounced as the complexity of the die increases. This wavy observation is likely to impact on the live span of the tools.

CONCLUSIONS

3.2 Conclusions

From the results obtained and their discussions, the following conclusions were drawn from the research carried out

- i. Die profile functions have been developed for extrusion of triangular, square, hexagonal, heptagonal and octagonal section from round billet using a mathematically contoured die profile. The procedure can also be used to develop other die profiles.
- ii. Solid CAD models of curved die profiles have been developed for extrusion of triangular, square, hexagonal, heptagonal, octagonal, T, L and H section.
- iii. FEM modeling have been carried out by using DEFORM-3D software using Aluminum alloy AA6063 as rigid plastic material for extrusion of triangular, square, hexagonal, heptagonal, octagonal, T, L and H section from round billet.
- iv. The load prediction, effective stress, the effective strain, the effective strain rate and the temperature distribution during deformation has been determined from FEM modeling.
- v. The extrusion pressure increases with increase in reduction, friction factor and die length.
- vi. There is no marked difference between the predictive loads for axisymmetric shapes.
- vii. The predictive loads for non- axisymmetric shapes are found to be higher than that of the axisymmetric shape.
- viii. The L-section has the highest extrusion load, followed by T-section and H-section given the least pressure

Reference

- [1] S.K. Sahoo, P.K. Kar, K.C. Singh, *A numerical application of the upper-bound technique for round-to-hexagon extrusion through linearly converging dies*, Journal of Materials Processing Technology 91 (1999) 105–110
- [2] S.K. Sahoo, P.K. Kar, K.C. Singh, *Upper-bound analysis of the extrusion of a bar of channel section from square/rectangular billets through square dies*, Journal of Materials Processing Technology 75 (1998) 75–80
- [3] K.P. Maity, P.K. Kar, N.S. Das, *A class of upper-bound solutions for the extrusion of square Shapes from square billets through curved dies*, Journal of Materials Processing Technology 62 (1996) 185- 190
- [4] R. Narayanasamy, R. Ponalagusamy, R. Venkatesan, P. Srinivasan, *An upper boundary solution to extrusion of circular billet to circular shape through cosine dies*, Materials and Design 27 (2006) 411–415
- [5] Frisch, J. and Mata-Pietric, E., *Experiments and the Upper Bound solution in Axisymmetric Extrusions*, In: Proceedings of the 18th International Machined Tool Design Research Conference, London, Macmillan, 1978, p. 55.
- [6] B.S. Altan, G. Purcek, I. Miskioglu, *An upper-bound analysis for equal-channel angular extrusion*, Journal of Materials Processing Technology 168 (2005) 137–146
- [7] J.S. Ajiboye, M.B. Adeyemi, *Upper bound analysis of die land length in cold extrusion*, Journal of Materials Processing Technology 177 (2006) 608–611
- [8] M.H. Paydara, M. Reihanihana, R. Ebrahimia, T.A. Deanb, M.M. Moshksara, *An upper-bound approach for equal channel angular extrusion with circular cross-section*, journal of materials processing technology 198 (2008) 48–53 57
- [9] D.K. Kim, J.R. Cho, W.B. Bae, Y.H. Kim, *Upper-bound analysis of square-die forward extrusion*, Journal of Materials Processing Technology 62 (1996) 242 - 248
- [10] S.K. Sahoo, *Comparison of SERR analysis in extrusion with experiment*, Journal of Materials Processing Technology 103 (2000) 293-303
- [11] Y.H. Kim, J.R. Choa, K.S. Kim, H.S. Jeong, S.S. Yoon, *A study of the application of upper bound method to the CONFORM process*, Journal of Materials Processing Technology 97 (2000) 153-157
- [12] W.A. Gordon, C.J. Van Tyne, Y.H. Moon, *Overview of adaptable die design for extrusions*, Journal of Materials Processing Technology 187–188 (2007) 662–667
- [13] N. Venkata Reddy, R. Sethurama, G.K. Lal, *Upper-bound and finite-element analysis of axisymmetric hot extrusion*, Journal of Materials Processing Technology 57 (1996) 14 22
- [14] M.K. Sinha, S. Deb, U.S. Dixit, *Design of a multi-hole extrusion process*, Materials and Design 30 (2009) 330–334
- [15] W. Johnson, *Experiments in the cold extrusion of rods of non-circular sections*, Journal of Mechanics and Physics of Solids 7 (1958) 37-44.
- [16] K. P. Maity, A. K. Rout, KaluMajhi, *computer-aided simulation of metal flow through curved die for extrusion of square section from square billet*, Presented in International Conference on Extrusion and Benchmark, Dortmund, Germany, 16-17 September, 2009
- [17] B.B. Basily, D.H. Sansome, *Some theoretical considerations for the direct drawing of section rod from round bar*, Int. J. Mech. Sci. 18 (1979) 201–209
- [18] V. Nagpal, T. Altan, *Analysis of the three-dimensional metal flow in extrusion of shapes. With the use of dual stream function*, in: Proceedings of the Third North American Metal Research Conference, Pittsburgh, PA, 1975, pp. 26–40
- [19] D.Y. Yang, C.H. Lee, *Analysis of three-dimensional extrusion of sections through curved dies by conformal transformations*, International Journal of mechanical science 20 (1978) 541–552
- [20] R. Prakash, O.H. Khan, *An analysis of plastic flow through polygonal converging dies with generalized boundaries of the zone of plastic deformation*, Int. J. Mach. Tool Des. Res. 19 (1979)1–9.
- [21] F. Gatto, A. Giarda, *The characteristics of three-dimensional analysis of plastic deformation according to the SERR method*, Int. J. Mech. Sci. 23 (1981) 129–148.
- [22] F. Halvorsen, T. Aukrust, *Studies of the mechanisms for buckling and waving in aluminum extrusion by use of a Lagrangian FEM software*, International Journal of Plasticity 22 (2006) 158–173
- [23] J. Lof, Y. Blokhuis, *FEM simulations of the extrusion of complex thin-walled aluminium sections*, Journal of Materials Processing Technology 122 (2002) 344–354
- [24] LIU Gang, ZHOU Jie, J DUSZCZYK, *Process optimization diagram based on FEM simulation for extrusion of AZ31 profile*, Trans. Nonferrous met. Soc. china18 (2008) 247-251
- [25] Tapas chanda, Jiezhou, JurekDuszczyk, *A comparative study on iso-speed extrusion and isothermal extrusion of 6061 Al alloy using 3D FEM simulation*, Journal of Material Processing Technology 114 (2001) 145-153
- [26] T. Chanda, J. Zhou, J. Duszczyk, *FEM analysis of aluminium extrusion through square and round dies*, Materials and Design 21 (2000) 323-335
- [27] Zhong Hu, Lihua Zhu, Benyi Wang, Zhuang Liu, YongchunMiao, PeiliangXie, ShengxingGu, Wei Sheng, *Computer simulation of the deep extrusion of a thin-walled cup using the thermo- mechanically coupled elasto-plastic FEM*, Journal of Materials Processing Technology 102 (2000) 128-137
- [28] K. D. Bouzakis, K. Efstathiou, G. Paradisiadis, A. Tsouknidas, *Experimental and FEM-supported investigation of wet ceramic clay extrusion for the determination of stress distributions on the applied tools” surfaces*, Journal of the European Ceramic Society 28 (2008) 2117–2127
- [29] Q. Li, C.J. Smith, C. Harris, M.R. Jolly, *Finite element investigations upon the influence of pocket die designs on metal flow in aluminium extrusion Part I. Effect of pocket angle and volume on metal flow*, Journal of Materials Processing Technology 135 (2003) 189–196
- [30] ZhiPeng, Terry Sheppard, *Simulation of multi-hole die extrusion*, Materials Science and Engineering A 367 (2004) 329–342
- [31] Gang Fang, Jie Zhou, JurekDuszczyk, *FEM simulation of aluminium extrusion through two-hole multi-step pocket dies*, journal of materials processing technology 209 (2009) 1891–1900
- [32] XinjianDuana, X. Velay, T. Sheppard, *Application of finite element method in the hot extrusion of aluminium alloys*, Materials Science and Engineering A369 (2004) 66–75
- [33] Geun-An Lee, Yong-TaekIm, *Analysis and die design of at-die hot extrusion process 2. Numerical design of bearing*

lengths, International Journal of Mechanical Sciences 44
(2002) 935–946

- [34] DEFORM TM 3D Version 6.1(sp2), *User's Manual*, Scientific Forming Technologies Corporation, 2545 Farmers Drive, Suite 200, Columbus, Ohio, 2008, 43235.

Nomenclature

English symbols (in alphabetical order)

A	half width of the product
D	diameter of the billet
L	length of the die
L_1	length of each side of the approximating polygon
m	friction factor on the die surface
N	unit vector normal to a surface
P_{av}	average extrusion pressure
R	radius of the billet
W	half-width of the billet
$\frac{p_{av}}{\sigma_0}$	Extrusion pressure
σ'	Flow stress
$\sigma_1, \sigma_2, \sigma_3$	principal stresses
ε'	Effective strain rate
$\varepsilon_1, \varepsilon_2, \varepsilon_3$	principal strain rate
θ	internal angle of the regular polygon

IJSER

Abbreviations

CAD	Computer aided design
ECAE	Equal-channel angular extrusion
FEM	Finite element method
SERR	Spatial elementary rigid region
3D	Three dimensional
KAVF	Kinematically-admissible velocity field
DEFORM	Design environment for forming
PR	Percentage reduction
U-B	Upper-bound